

# Optical Central Clock Distribution for MIMO-Enabled, Millimeter Wave Wireless Interconnects

Shu-Hao Fan, Daniel Guidotti, Arshad Chowdhury, Hung-Chang Chien, Gee-Kung Chang

School of Electrical and Computer Engineering, Georgia Institute of Technology, Atlanta, GA 30332 USA  
shfan@gatech.edu

**Abstract:** We propose a novel optical clock distribution scheme for MIMO-enhanced wireless interconnects. Low-power, error-free, multi-gigabit wireless transmission has been demonstrated by employing centrally distributed optical clock.

© 2011 Optical Society of America

**OCIS codes:** (200.0200) Optics in Computing; (200.4650) Optical Interconnects

### 1. Introduction

As the processing power of silicon electronics increases every year, the focus of high-performance computing (HPC) technology moves from improving the sheer speed of transistors to the memory access speed of the interface bus. As the von Neumann bottleneck states, the memory access throughput can hinder the overall computational speed in today's computing architecture. The multi-core streaming processing solution, such as the 448-core nVidia Tesla C2000-Series general-purpose graphics processing unit (GPGPU), is demanding even faster (over 1000GT/s) memory access speed. In general, large-volume memory blocks required for multi-core computing are usually outside the processor chip, the meager bandwidth-distance product of copper wires will soon not meet the demands of the HPC units.

The limitation of copper is mainly due to the path loss at the high frequency. At 20 GHz, a typical differential pair of copper on a FR-4 board has the loss of 1.0 dB/cm whereas the low-loss liquid-crystal-polymer substrate still has around 0.7dB/cm [1]. High cross-talk, RC delays, and radiation loss also restricts the copper transmission distance at very high speed. Therefore, the optical interconnect have been proposed to replace the copper wire because of its extremely low loss and negligible cross-talk for the adjacent waveguides. Approximately 0.02dB/cm along polymer waveguides was reported by many major companies. However, the doubts about the yield and failure rate of vertical-cavity surface emitting lasers (VCSEL) are still not clarified, especially for exascale HPC units, which require thousands of interconnecting channels working reliably. Moreover, the problem of optical alignment for multi-channel interconnects slows down both the reliability and cost progresses of the HPC systems.

In the past, wireless interconnects have not been taken seriously until recently because of the growing demand and component maturity of the millimeter-wave (mm-Wave) communication technology for wireless personal area networks (WPANs) such as wireless-HD and IEEE 802.15.3c. The new mmWave technology not only allows multi-gigabit interconnects but also shrinks the size of the radio-frequency (RF) module to a smaller footprint [2]. Using RF signals to transmit data can have better spectral efficiency than baseband signals because of the in-phase and quadrature (I/Q) modulation. For example, a simple duobinary-PSK can have the spectral efficiency of 4bit/s/Hz. In addition, since the path loss of wireless transmission is only inversely proportional to the square of the distance, the path loss of the mmWave transmission in the air is much lower than the copper wire after a certain distance. However, as the wireless inter-chip interconnects draws more and more attention recently, there are very few

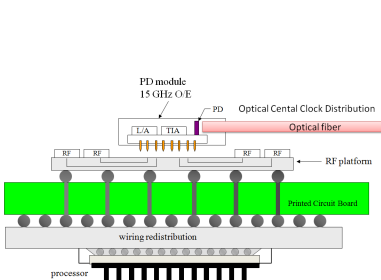


Fig. 1. Schematic of the OCCD MIMO RF modules for inter-chip interconnects.

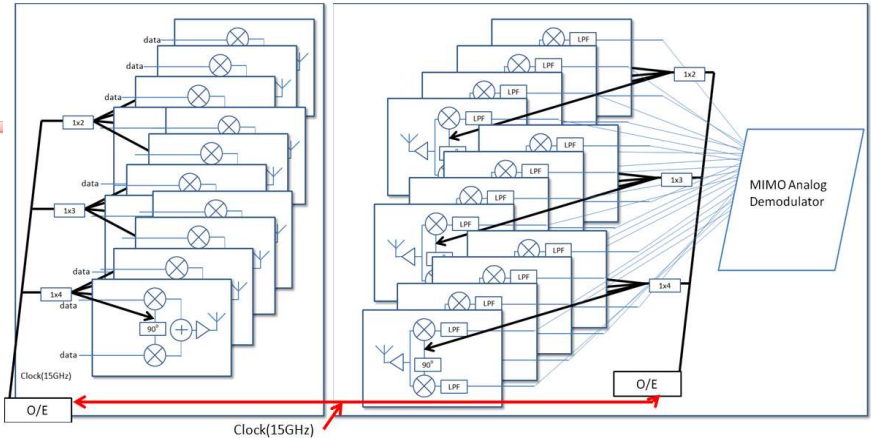


Fig. 2 FDM-MIMO Transmitter and Receiver Design with OCCD

discussions about the interference between different wireless transmitter-receiver pairs. After all, the interference is inevitable when the transmission distance is getting longer. Therefore, we proposed the spatial multiplexing multi-input-multi-output (MIMO) transmission, which takes advantages of the interference to increase the data rate over the same RF band. And, the central frequency of the RF is globally synchronized by the optical fiber by the optical central clock distribution (OCCD).

As shown in Fig. 1, all the RF frequency comes from the same source, which distributes the clock by optical fibers. The carrier frequency of each RF modules is simultaneously synchronized. This brings two advantages over conventional wireless interconnects. First, it saves the phase-lock-loops (PLLs) and local oscillators, and therefore, it reduces the power of RF modules dramatically [3]. Second, it reduces the complexity of phase-locking in the MIMO transmission. The spatial multiplexing MIMO transmits RF signals with various location-dependent phases at the same time, making the conventional PLL difficult to work. Frequency-division multiplexing (FDM) can be also easily deployed by the OCCD, as shown in Fig. 2 to reduce the complexity and difficulty of the MIMO demodulation. The receiver then down-converts the RF signals to the baseband. Because the wireless condition is rigorously fixed in the HPC racks, the demodulation of the MIMO can be achieved by a simple analog circuit, instead of power-hungry digital signal processing.

## 2. MIMO Analog Demodulation

To illustrate the principle of MIMO analog demodulation, we can simplify the MIMO transmission to one-dimensional array. The pitch distance between two transmitter/receiver antennas is  $d$ , while the distance and angle of the transmitter to the receiver is  $R$  and  $\theta$  respectively. Assuming the arrival time difference between any two transmitter-receiver pairs is much smaller than the data bit period, hence the received signal can be modeled as a one-tap operation. In our design, we assume that the system has unlimited bandwidth, thus the received signal,  $\vec{y} = [y_1 y_2 y_3 \dots]^T$  can be modeled by

$$\vec{y} = H\vec{x} + \vec{w}, \quad (1)$$

where  $\vec{x}$  and  $\vec{y}$  are the transmitted and received vector respectively, and  $\vec{w}$  is the noise vector for each receiver. The channel matrix  $H$  describes amplitude and phase relation between each transmitter-receiver pair. Therefore, the receiver can recover by the original signal as long as the channel matrix is known, which is not difficult because all the antenna locations are fixed:

$$\hat{\vec{x}} = H^{-1}\vec{y} + H^{-1}\vec{w}. \quad (2)$$

This demodulation function of  $\vec{y}$  is simply a series of additions and scalar multiplications, which can be achieved by a simple analog circuit in the baseband. The performance of the MIMO analog demodulation, however, depends on the channel matrix  $H$ . As expressed in Eq. (2), If the condition number of  $H$  is high, the noise term will be amplified to degrade the accuracy of the estimation. The condition number of  $H$  depends on the angle  $\theta$  and most sensitive to the distance ratio  $R/d$ . We ran a simulation of a 2x2 MIMO OOK transmission with  $R=15\text{cm}$ ,  $\theta=75^\circ$  in the line-of-sight ray tracing condition. The signal-to-noise ratio is defined by:

$$SNR = E \left[ \frac{\vec{x}^* H^* H \vec{x}}{\vec{w}^* \vec{w}} \right], \quad (3)$$

where  $(.)^*$  represents the Hermitian matrix. Figure 3 shows the simulation results of the BER versus SNR. With smaller value of  $d$ , the condition number increases and the BER performance is hereby degraded. Figure 4 shows the simulation results of 2x2, 4x4, 6x6, and 8x8 MIMO transmissions with  $d=1.0\text{cm}$ . It is observed that the BER performance is mainly determined by the condition number of  $H$ . As a result, to transmit data over ill-conditioned

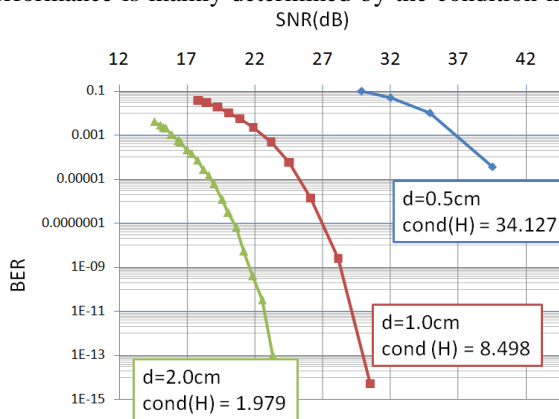


Fig. 3 FDM-MIMO Transmitter and Receiver Design with OCCD

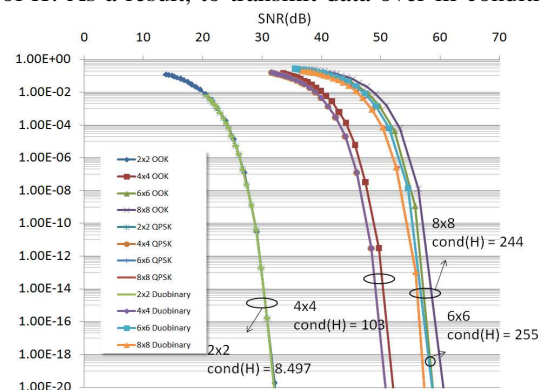


Fig. 4. The diagram of BER versus SNR for modulation formats and antenna number. The pitch distance is fixed at 1 cm. Cond(H): condition number of the channel matrix H.

situation (such as  $R/d$  is too high or the angle is too large) a pre-scrambler can be added before the RF transmitters to the corresponding channel matrix  $H$ .

### 3. Experimental Results

In order to quantify the performance of the MIMO analog demodulation, we set up a 60-GHz 2x2 MIMO experimental testbed. Due to limited availability of equipment in our lab, we only generated two transmitted data by the optical carrier suppression, as shown in Fig. 6. The optical 60-GHz signal was first generated by a phase modulator and an optical interleaver. Then, the optical mmWave signal was separated by two different-length fibers to represent two independent data. Two o/e modules converted the optical signals to RF signals and sent them to the air by two 15-dBi antennas. At the RF receivers, two 60-GHz in-phase down-converters were used to detect the signal. The 2x2 MIMO subsystem located the four antennas in a position such that the receiver saw a 90-degree phase shift from the two incoming signals from the two transmitters. The amplitudes of the two incoming signals were adjusted by the electrical amplifiers so the receivers saw approximately the same amplitude. Therefore, the normalized channel matrix  $H$  can be depicted by

$$H = \begin{bmatrix} 1 & j \\ j & 1 \end{bmatrix}. \quad (4)$$

The outputs of the two down-converters were set to be  $\varphi_{L1} = 0$ ,  $\varphi_{L2} = \pi/2$ , as shown in Fig. 6. Neglecting the noise term, the outputs are

$$\hat{\tilde{x}} = \text{Re} \left\{ \begin{bmatrix} 1 & -j \\ -j & 1 \end{bmatrix} \begin{bmatrix} 1 & j \\ j & 1 \end{bmatrix} \tilde{x} \right\} = \text{Re}\{\tilde{x}\}. \quad (5)$$

In Fig. 6, it shows the transmitted and received 9-Gb/s x 2 duobinary signals, occupying only 2.25-GHz baseband bandwidth. However, in lack of a duobinary decoder, we can only measure the BER performance of 2-Gb/s x 2 OOK signals. The pitch between the two transmitter antennas is about 10 cm and the transmission distance is 50 cm. The optical SNR (OSNR) is estimated by an optical spectrum analyzer (OSA) at 0.1nm resolution. Error-free 2x2 MIMO OOK transmission can be detected after 50 cm at OSNR of 29.6dB. The penalty of the 2x2 MIMO transmission to the single-input-single-output (SISO) is due to the imperfection of the phase orthogonality and the RF component bandwidth around 60 GHz.

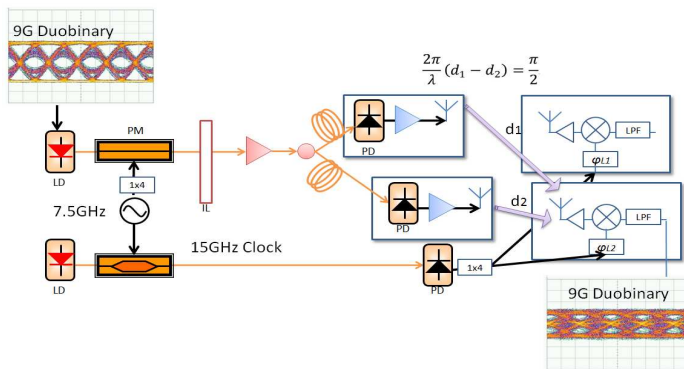


Fig. 5. The experimental setup of the 2x2 MIMO fixed-location transmission. PM: phase modulator; PD: photodiode; LD: laser diode; LPF: low-pass filter; IL: 33GHz/66GHz optical interleaver

### 3. Conclusions

We propose an optical central clock distribution (OCCD) scheme for millimeter wave wireless interconnects over ultra-short distance that enables MIMO-based high-speed transmission with a simple demodulation scheme. Wireless transmission of 9-Gb/s x 2 duobinary using 2x2 MIMO has been successfully demonstrated. The BER measurement of 2-Gb/s x 2 OOK 2x2 has been carried out to verify the error-free transmission at OSNR of 29.6dB. In view of the increasing demand of high-speed memory access for high performance computers (HPCs), we believe that the MIMO-enabled OCCD is a promising solution of inter-chip interconnects for next generation HPC architecture.

### 4. References

- [1] R. Lollipara, et. al., "Evaluation of a module based memory system with an LCP flex interconnect," IEEE 59<sup>th</sup> ECTC, pp. 1200-1206, 2009.
- [2] W.-H. Chen, et. al., "A 6-Gb/s Wireless Inter-Chip Data Link Using 43-GHz Transceivers and Bond-Wire Antennas," IEEE Journal of Solid-State Circuits, vol. 44, no. 10, pp. 2711-2721, 2009.
- [3] D. Guidotti, et. al., "Toward a 60-GHz wireless, low-power, high-throughput memory access system," Microwave and Optical Technology Letters, vol. 51, no. 12, pp. 2969-2973, 2009.

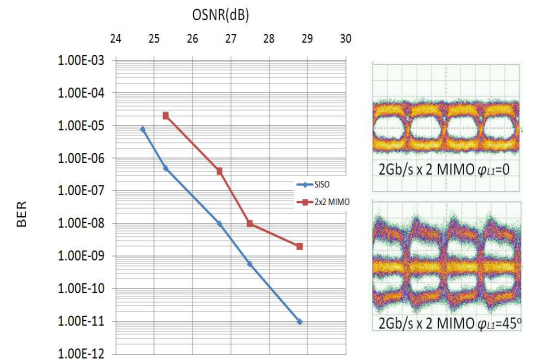


Fig. 6. The experimental results of the BER performance versus OSNR of the 2Gb/s x 2 OOK MIMO transmission. The insets on the right side shows the measured 2x2 MIMO error-free eye diagram at OSNR=29.6dB.